Molecular Vision 2025; 31:85-97 <http://www.molvis.org/molvis/v31/85>
Received 14 October 2024 | Accepted 26 March 2025 | Published 28 March 2025

DNA methyltransferase 1 regulates epithelial cell functions in corneal and eyelid development

Antonius Christianto,[1] Maureen Mongan,[1] Bo Xiao,[1] Qin Wang,[1] Alvaro Puga,[1] Michael L. Robinson,[2] Ying Xia[1]

[1]Department of Environmental and Public Health Sciences, University of Cincinnati College of Medicine, Cincinnati, OH; [2]Department of Biology, Miami University, Miami, OH; Dr. Christianto currently at School of Life Sciences and Technology, Institute Teknologi Bandung, Bandung 40132, Indonesia; Dr. Wang is currently at Nonclinical Safety Assessment, BeiGene (Beijing) Co. Ltd, Beijing 100020, China

Purpose: DNA methyltransferase 1 (DNMT1) is a crucial enzyme for the development of the retina and lens in the eye, but its roles in the cornea and eyelids are yet to be investigated.
Methods: Ocular surface epithelium (OSE)-specific *Dnmt1* knockout mice, denoted as *Dnmt1*$^{\Delta OSE}$, were generated. Prenatal eye tissues were characterized by hematoxylin and eosin staining; DNMT1 expression, DNA methylation, epithelial differentiation and cell–cell junctions were determined by immunohistochemistry; proliferation was assessed by 5-ethynyl 2′-deoxyuridin labeling and apoptosis evaluated by terminal deoxynucleotidyl transferase dUTP nick-end labeling assay. Keratinocytes derived from *Dnmt1*$^{F/F}$ mice were infected with adenoviruses carrying either green fluorescent protein or Cre recombinase to obtain wild-type and *Dnmt1*-deficient cells. In these cells, *Dnmt1* expression and epithelial terminal differentiation were evaluated by real-time PCR and/or western blotting; adherence junction and apoptosis were assessed by immunohistochemistry; proliferation was determined by 5-ethynyl 2′-deoxyuridin labeling; transcription factor activities were determined by luciferase reporter assays.
Results: The abundant DNMT1 expression and cytosine methylation (5meC) detected in the ocular surface epithelia of wild-type embryos were largely diminished in that of *Dnmt1*$^{\Delta OSE}$ embryos. Besides lens degeneration, the *Dnmt1*$^{\Delta OSE}$ fetuses had severe abnormalities of the cornea and eyelids. The surface epithelial cells and stromal keratocytes in the knockout corneas were distorted and the eyelids failed to fuse in the knockout embryos, resulting in an eye-open-at-birth phenotype. At the cellular level, DNMT1-deficient OSE had normal proliferation but increased apoptosis and aberrant cell junctions. In addition, the knockout corneal epithelia failed to express corneal-specific keratin 12, and the knockout eyelid epithelia had increased expression of keratin 10, indicating accelerated terminal differentiation. In vitro studies validated that DNMT1 was required for epithelial cell survival, terminal differentiation and cell junctions, and further identified signaling pathways aberrantly activated by its ablation.
Conclusion: DNMT1 maintains survival and differentiation of corneal and eyelid epithelium for the development of the eye.

DNA methylation involves covalent addition of a methyl group to the cytosine of DNA, a prevalent epigenetic modification throughout the genome and crucial for regulation of gene expression [1–3]. This event is catalyzed by DNA methyltransferases (DNMTs). In mammals, there are three DNMTs—DNMT1, DNMT3A and DNMT3B [4]. While DNMT3A and DNMT3B have unique and overlapping roles in de novo methylation, DNMT1 is a key enzyme responsible for preserving the methylation signatures in successive cell generations. Specifically, DNMT1 acts on hemimethylated DNA and copies the parental methylation status to the daughter strand following DNA replication [5,6]. Through these activities, DNMT1 regulates fundamental biological processes, such as inactivation of nonallelic X chromosome, sustaining imprinting signatures and preserving genome stability [7], and is required for normal embryonic and fetal development [8].

There is compelling evidence supporting the roles of DNMT1 in development. In mice, DNMT1 knockout causes severe developmental abnormalities, leading to early embryonic death, accompanied by global DNA hypomethylation, aberrant expression of imprinted genes and chromosomal instability [5,9]. Studies of conditional *Dnmt1* knockout mice have revealed additional cell type-specific roles of the gene products in the formation of different tissues. For example, muscle-specific *Dnmt1* deletion results in defective myogenic differentiation and myoblast fusion. The promoter of *Id-1* is hypomethylated in DNMT1-deficient progenitors, leading to increased expression of Id-1, a transcription factor that negatively regulates myogenesis [10]. Loss of DNMT1 in the intestine causes DNA damage, premature differentiation,

Correspondence to: Ying Xia, Department of Environmental and Public Health Sciences, University of Cincinnati, College of Medicine, Cincinnati, OH; email: ying.xia@uc.edu

apoptosis and subsequent loss of nascent villi [11]. Moreover, depletion of DNMT1 in keratinocytes promotes the early exit of progenitor status, causing premature differentiation and eventually loss of skin tissues [12].

In the eye, DNMT1 is required for neural retina differentiation. Retinal-specific *Dnmt1* deletion results in compromised neuronal differentiation and rapid cell death [13,14]. In the lens, DNMT1 is required for lens epithelial cell survival but is dispensable for primary lens fiber differentiation [15]. Little is known about the developmental roles of DNMT1 in other ocular tissues besides the retina and lens. Here, we investigated cornea and eyelid development through mouse analysis, in which the *Dnmt1* gene was specifically ablated in the ocular surface epithelium (OSE). Our data showed that DNMT1 was required for survival and differentiation programs of corneal and eyelid epithelia. Thus, DNMT1 inactivation, commonly caused by exposure to environmental chemicals and anticancer agents, could lead to congenital diseases affecting the cornea and eyelid [16–19].

METHODS

Animals: Dnmt1$^{F/F}$/*Le-Cre*$^{TG/-}$ females were crossed with *Dnmt1*$^{F/F}$ males and the *Dnmt1*$^{F/F}$ embryos/fetuses with or without a *Le-Cre*^{TG} allele, denoted as *Dnmt1*$^{\Delta OSE}$ or wild-type pups, respectively, were collected for analyses as described before [15]. Genotype was determined by PCR using tail-cut genomic DNA and the primers listed in Appendix 1. Animals were housed in a pathogen-free vivarium in accordance with institutional policies. All animal experiments were approved in advance by the Institutional Animal Care and Use Committee at the University of Cincinnati College of Medicine.

Keratinocyte and stable cell lines: Mouse keratinocytes derived from *Dnmt1*$^{F/F}$ mice were cultured and maintained in Keratinocyte Serum Free Medium without Calcium Chloride (10,725-018, Gibco, Thermo Fisher Scientific, Waltham, MA) media, as described before [20]. To develop stable reporter cell lines, the *Dnmt1*$^{F/F}$ cells were infected with lentivirus carrying the pathway luciferase reporters purchased from LipExoGen Biotech (Appendix 2); stable cells were obtained following Blasticidin (R21001, Thermo Fisher Scientific) selection. The cells were subsequently infected with adenoviruses expressing either green fluorescent protein (Ad-GFP) or GFP plus Cre recombinase (Ad-GFP-Cre, or Ad-Cre) at 5 IU for 48 h to generate wild-type and *Dnmt1*-knockout (deficient) keratinocytes, respectively.

Histology and immunofluorescent staining: The heads of appropriately euthanized dams were collected and fixed in 4% paraformaldehyde (PFA) at 4 °C overnight. Tissues were embedded in paraffin and sectioned at 5 µm with a microtome (MT-980, Research & Manufacturing Co., Inc., Tucson, AZ). Selected serial tissue sections were subjected to hematoxylin (ES701, Azer Scientific, Morgantown, PA) and eosin (ES709, Azer Scientific) staining, and images were captured using Zen 3.1 (Blue edition) under bright-field light microscopy (Zeiss AXIO Scope A1, Göttingen, Germany) at different magnifications.

For immunohistochemistry, tissue sections representing the center of the eye were deparaffinized and immersed in boiled 10 mM citrate buffer (pH 6.0) for 30 min for antigen retrieval. The sections were blocked with phosphate-buffered saline/tween (PBST) containing 5% normal goat serum (PCN5000, Gibco, Thermo Fisher Scientific) for 1 h at room temperature and incubated with a diluted primary antibody overnight at 4 °C followed by secondary antibodies and Hoechst 33,342 (H1399, Thermo Fisher Scientific) staining. The list of antibodies and dilutions for each antibody is listed in Appendix 3. Images were captured using a confocal laser scanning microscope (Zeiss AXIO Observer Z1 LSM 700).

For cultured cell immunofluorescent staining, the *Dnmt*$^{F/F}$ keratinocytes grown on cover glass were infected with Ad-GFP or Ad-Cre in Defined Keratinocyte Serum Free Medium (10,785-012, Gibco, Thermo Fisher Scientific) as described before [20]. After washing with PBS, the cells were fixed with 4% PFA at 4 °C for 20 min followed by incubation with a blocking solution of PBST containing 0.25% bovine serum albumin (BSA; A2153, Sigma-Aldrich, St. Louis, MO) for one hour at room temperature. Immunostaining was performed as that described for tissue sections.

Apoptosis and proliferation: To determine apoptosis, the tissue sections were subjected to terminal deoxynucleotidyl transferase dUTP nick-end labeling assays using the ApopTag® Plus in situ Apoptosis Fluorescein Detection Kit (S7111, Millipore Sigma, Temecula, CA) following the manufacturer's protocol. Keratinocytes grown on cover glass with Ad-GFP and Ad-Cre infection as described above were examined by immunofluorescent staining with anti-Caspase-3 (CST 9663S, Cell Signaling Technology, Danvers, MA) as the primary antibody, Alexa Fluor™ 594 Goat anti-Rabbit IgG (H$^+$L; A11012, Invitrogen) as the secondary antibody and Hoechst 33,342.

To determine proliferation, 2 h after intraperitoneal injection/incubation with 5-ethynyl 2′-deoxyuridine (EdU; Component A, 5 mg/kg b.w. or 10 µM in growth media), embryos/fetuses were collected from pregnant mice and cultured cells harvested. Tissue sections and keratinocytes were infected with Ad-GFP/Ad-Cre and subjected to an iClick™ EdU Andy Fluor™ 594 Imaging Kit (A005, ABP

Biosciences, Beltsville, MD) following the manufacturer's protocol.

Cell apoptosis and proliferation were observed, and images were captured with a Zeiss AXIO Observer Z1 LSM 700 microscope. The staining positive cells were quantified and the percentage of positive staining was calculated versus total cells. The results represent data from at least three sections per embryo and three embryos/genotypes of different litters; data from cultured keratinocytes were quantified in three samples, and only green cells positive for Ad-GFP or Ad-Cre infection were included in quantification.

RNA isolation, reverse transcription and quantitative real-time PCR: Total RNA was extracted from cultured keratinocytes with a PureLink® RNA Mini kit (121,830, Invitrogen, Waltham, MA) following the manufacturer's protocol. A total of 1 µg RNA was subjected to reverse transcription using a SuperScript™ IV First-Strand Synthesis System (18091050, Invitrogen). The cDNA was mixed with gene-specific primers and SYBR Green QPCR Master Mix, and subjected to quantitative real-time PCR an MX3000p thermal cycler system (Agilent Technologies, St. Clara, CA). Relative gene expression was calculated by the comparative ΔΔCt-method normalized to the constitutively expressed housekeeping gene, *Gapdh*. Data represented duplicates of at least three independent samples. Primer sequences are listed in Appendix 4.

Western blotting: Cells grown on a culture dish were lysed with RIPA buffers (0.5M EDTA pH 8, 0.1% SDS, 1% NP-40, 5M NaCl, 1M Tris-HCl pH 7.6, 2.5 g NaDOC, protease inhibitor). A total of 50 µg cell lysates were subjected to SDS PAGE, followed by western blotting using anti-DNMT1 and anti-β-actin. Sources and dilutions of the primary and secondary antibodies are listed in Appendix 3. Immunoblotting was detected by chemiluminescence and images were captured with a Gel Imaging System (UVP Transilluminator, Analytik Jena Company, Upland, CA). Signals were quantified by ImageJ software and the signal intensity of DNMT1 was compared with that of β-actin as the loading control.

Luciferase activities: Ad-GFP– or Ad-Cre–infected *Dnmt1*$^{F/F}$ reporter cells in 24-well plates were lysed and the activity of luciferase was measured using a luciferase assay system (Rapid detection of Firefly Luciferase activity, E1500, Promega, Madison WI). Relative luciferase activities were quantified after normalization with the cell's total protein. The results represent duplicate data from four biologic samples of each adenovirus transfection, Ad-GFP and Ad-Cre.

Statistical analysis: At least three independent samples were used in all experiments for data analysis. Statistical analysis was performed using a Student's two-tailed paired *t* test for comparison between groups. The exact number of biologic replicates and statistical analysis used for each experiment are included in the figure legends. Values of $p < 0.05$ (*), $p < 0.01$ (**) and $p < 0.001$ (***) were considered statistically significant.

RESULTS

Abnormal corneal and eyelid development in Dnmt1 ocular surface epithelium knockout mice: We crossed *Dnmt1*$^{F/F}$ mice with mice carrying one *Le-Cre* allele that expressed Cre recombinase in the OSE [21]. The resultant *Dnmt1*$^{F/F}$*/Le-Cre* mice, denoted as *Dnmt1*$^{\Delta OSE}$, should have *Dnmt1* specifically knocked out in the OSE, whereas the *Dnmt1*$^{F/F}$ littermates were considered as wild-type controls. We collected E15.5 embryos to determine DNMT1 expression. In the wild-type embryos, DNMT1 was expressed ubiquitously in the epithelial and stromal cells of the ocular surface tissues, including the lens, cornea and eyelids. In *Dnmt1*$^{\Delta OSE}$ embryos, while DNMT1 expression was still abundant in stromal cells, it was largely absent in the OSE (arrowheads, Figure 1A). Concurrently, DNMT1-mediated 5-methylcytosine (5meC) was abundant in the OSE of the wild-type embryos but undetectable in that of the knockout embryos (arrowheads, Figure 1B).

To determine whether defective DNMT1 expression and DNA methylation affected eye development, we examined the histology of wild-type and *Dnmt1*$^{\Delta OSE}$ eyes at E14.5–E16.5, encompassing the late embryogenic to early fetal developmental phases. Consistent with a previous report [15], OSE DNMT1 ablation caused lens degeneration. The knockout lens lost capsule epithelial cells and was smaller in size compared with those of wild-type embryos (Figure 2). The knockout lens was also frequently associated with anterior cell clusters (Figure 2, hash #) fused to the corneal endothelium as well as posterior debris located between the lens and the retina.

Unlike the *Dnmt1*$^{\Delta OSE}$ lens, in which degeneration was evident in the E14.5 embryos, the knockout cornea and eyelids at this stage appeared to be normal; however, they exhibited clear abnormalities from E15.5 onward. The knockout corneas protruded anteriorly and became thicker and the knockout eyelids failed to fuse, leaving the corneal surface exposed at E16.5. In contrast, the wild-type had thinner corneas and their upper and lower eyelids were fused over the cornea. Corneal and eyelid abnormalities were observed only in *Dnmt1*$^{F/F}$*/Le-Cre* but not *Dnmt1*$^{+/F}$*/Le-Cre* fetuses, indicating that *Dnmt1* deletion was autosomal recessive for corneal and eyelid defects (Appendix 4). These observations also suggest that Le-Cre expression is not responsible for the defective phenotypes observed in *Dnmt1*$^{F/F}$*/Le-Cre* pups.

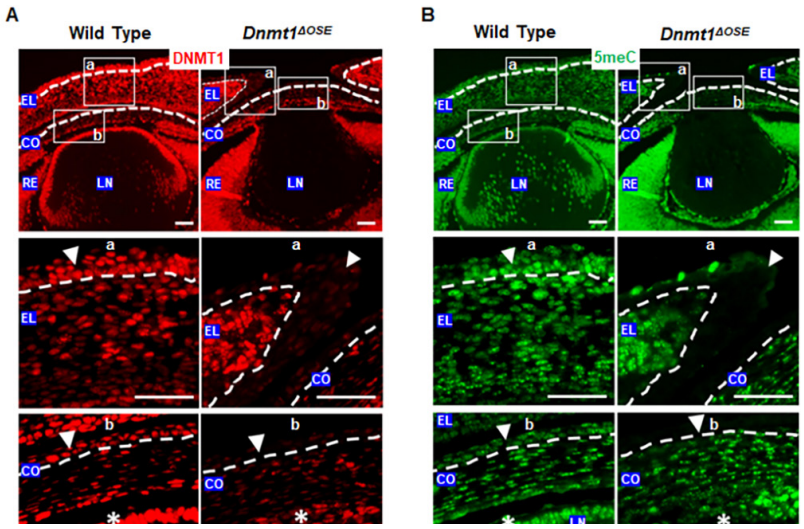

Figure 1. Defective DNA methyltransferase 1 expression and DNA methylation in the ocular surface epithelium of *Dnmt1*$^{\Delta OSE}$ embryos. Wild-type and *Dnmt1*$^{\Delta OSE}$ E15.5 embryonic eye sections were examined by immunostaining for (**A**) DNMT1 and (**B**) 5meC. Dashed lines indicate the epithelial basement membrane. Top panels, low magnification images; middle and lower panels, higher magnifications of selected areas of (a) the eyelid and (b) the cornea, respectively. Arrowheads point to the eyelid epithelium in (a) and the corneal epithelium in (b), the asterisk marks the lens epithelium in (b). EL, eyelid; CO, cornea; RE, retina; LN, lens. Images are representative of at least three mice/genotypes. Scale bars: 50 µm.

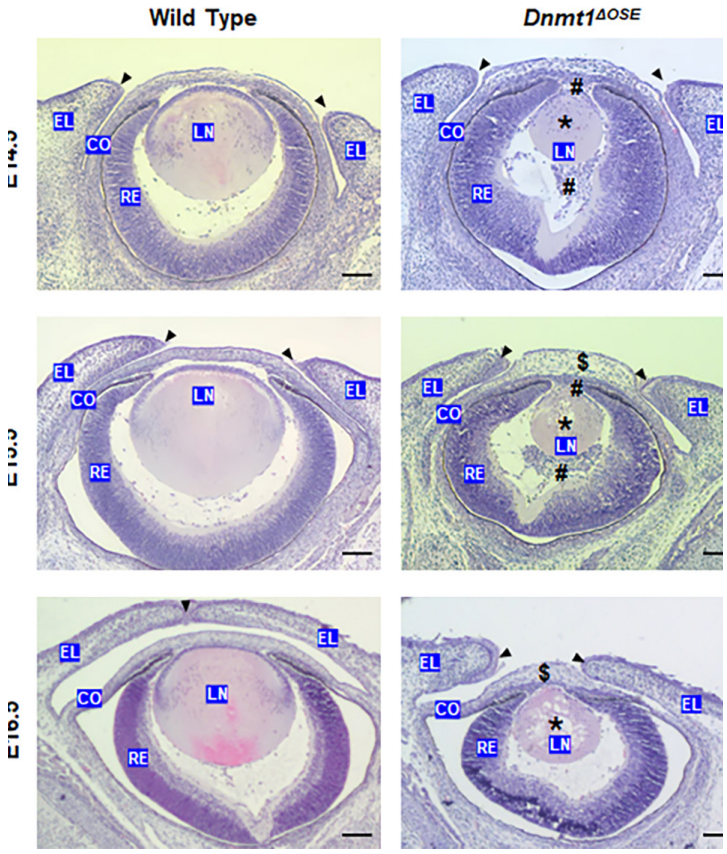

Figure 2. Abnormalities of the eyelids, cornea and lens in *Dnmt1*$^{\Delta OSE}$ eyes. Wild-type and *Dnmt1*$^{\Delta OSE}$ eye sections at the embryonic days indicated were subjected to hematoxylin and eosin staining. Arrowheads point to the eyelid tip leading edge. $ indicates corneal edema, * indicates the degenerated lens and # indicates the cell clumps above and below the degenerative lens in the *Dnmt1*$^{\Delta OSE}$ eyes. EL, eyelid; CO, cornea; RE, retina; LN, lens. Images are representative of at least three mice/genotypes. Scale bars: 50 µm.

Thus, DNMT1 expression in the OSE is required for corneal and eyelid development at late embryogenesis in addition to its role in lens development.

DNA methyltransferase 1 is required for corneal epithelial organization and differentiation: During embryonic development, the corneal epithelium is comprised of uniformed epithelial cells aligned in two layers above the basement membrane. We detected well-organized epithelial layers in the corneas of wild-type fetuses; however, we found irregular-shaped epithelial cells arranged in a distorted pattern with large intercellular spaces in the corneas of knockout fetuses (arrows, Figure 3A). Some of the basal *Dnmt1*$^{\Delta OSE}$ corneal epithelial cells were detached from the basement membrane (asterisks, Figure 3A). The wild-type and *Dnmt1*$^{\Delta OSE}$ corneal stroma was also strikingly different. The corneal stroma of wild-type fetuses was packed with residential keratocytes aligned parallel to the basement membrane, whereas the corneal stroma of *Dnmt1*$^{\Delta OSE}$ fetuses, filled with irregular-shaped keratocytes, was nearly twice the thickness of that in wild-type (Figure 3A,B). Similar observations were made in both E15.5 and E16.5 embryos/fetuses (Figure 3 and Appendix 4).

The stromal thickness in *Dnmt1*$^{\Delta OSE}$ embryos was not due to an increased number of keratocytes, but corresponded to larger intercellular spaces (Figures 3A,B). These observations led to the hypothesis that DNMT1 loss impairs the barrier function of the corneal epithelium, which in turn causes fluid accumulation and edema of the corneas. To test the hypothesis, we determined cell–cell junctions that constituted the epithelial barrier by establishing tight cell connections. One of the cell junctions is mediated by E-cadherin (E-Cad), a transmembrane protein and a key component of the adherens junctions to establish cell–cell contacts [22]. While E-Cad was detected on the plasma membrane of corneal epithelial cells, apparent differences were found between wild-type and *Dnmt1*$^{\Delta OSE}$ (Figure 3C). E-Cad was evenly distributed on the plasma membrane at the cell–cell and cell–basement membrane junctions in wild-type corneas. It was also

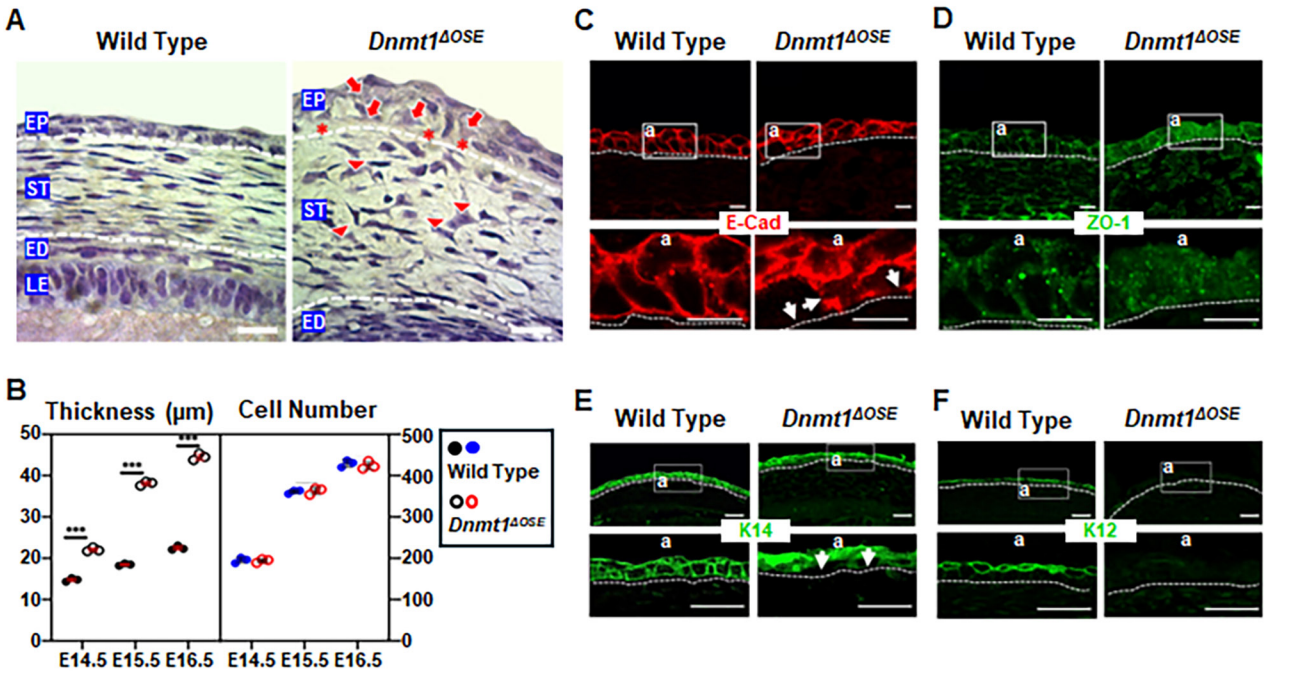

Figure 3. DNA methyltransferase 1 maintains cornea integrity and differentiation. **A**: High magnification of hematoxylin and eosin-stained images of the corneas of wild-type and *Dnmt1*$^{\Delta OSE}$ E16.5 embryos. The dashed lines indicate corneal stroma junctions with the epithelium and endothelium. Arrows point to abnormal-shaped epithelial cells, asterisks show basal cells detached from the basement membrane and arrowheads point to the abnormal stromal cells in the *Dnmt1*$^{\Delta OSE}$ cornea. EP, epithelium, ST, stroma, ED, endothelium. **B**: Measurement of the stroma thickness (left) and quantification of keratocytes (right) in wild-type and *Dnmt1*$^{\Delta OSE}$ corneas. Values are mean ± s.e.m. of three embryos/genotype. ***p < 0.001 (two-tailed Student *t* test). Immunohistochemistry of the corneas epithelium in E15.5 embryos using (**C**) anti-E-cadherin (E-Cad), (**D**) anti-ZO-1, (E) anti-K14 and (F) anti-K12 at low (upper panels) and high (lower panels) magnifications of the selected areas (a, lower panels). Dotted lines indicate corneal epithelial basement membranes. White arrows indicate epithelial cell detachment from the basement membrane. Images are representative of at least three mice/genotypes. Scale bars: 10 μm for (**A**), (**C**) and (**D**). 30 μm for (**E**) and (**F**).

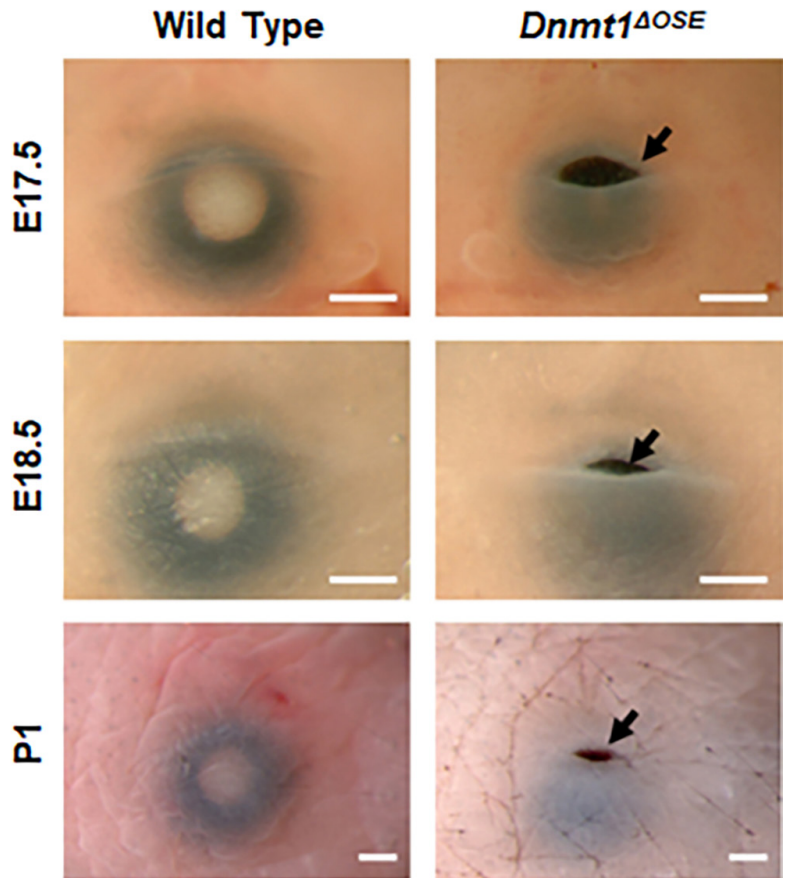

Figure 4. Eye-open phenotypes of *Dnmt1*$^{\Delta OSE}$ mice. Photographs of wild-type and *Dnmt1*$^{\Delta OSE}$ eyes at different developmental stages. Wild-type pups showed eyelid fusion but *Dnmt1*$^{\Delta OSE}$ pups displayed eye-open phenotypes (arrows). Images are representative of at least three mice/genotypes. Scale bar: 1 mm.

located at the cell–cell junction in *Dnmt1*$^{\Delta OSE}$ corneas but was missing on ectopic spots between the epithelial and basement membranes (arrows, Figure 3C). Another key cell junction is mediated by Zonula Occludens-1 (ZO-1), also a transmembrane protein and a component of the tight junction complexes that regulate paracellular movement of ions and solutes between cells [23]. ZO-1 proteins were located predominantly on the plasma membrane of the corneal epithelium in wild-type embryos; however, they displayed diffused distribution throughout the cytosol in the knockout corneal epithelium (Figure 3D).

The corneal epithelium comprises stratified squamous epithelium that express distinct keratin intermediate filaments during embryonic development [24]. Keratin 14 (K14) is the basal epithelial cell marker expressed in all epithelial cells as early as E9.5 [25], whereas K12, a corneal-specific keratin essential for epithelial integrity and function, starts to express at E15.5 [26]. Examination of these keratins in wild-type and *Dnmt1*$^{\Delta OSE}$ E15.5 embryos showed that K14 was evenly distributed on the plasma membrane of wild-type corneal epithelial cells but exhibited an uneven and sporadic distribution and was largely absent in basal cells above the basement membrane of *Dnmt1*$^{\Delta OSE}$ corneas (Figure 3E). Moreover, K12, located on the plasma membrane of the suprabasal corneal epithelial cells in wild-type embryos, was completely undetectable within the corneas of *Dnmt1*$^{\Delta OSE}$ embryos (Figure 3F). Together, our data indicate that DNMT1 is required to maintain the integrity and differentiation of the corneal epithelium, and that its deficiency causes a disorganized epithelium as well as stroma and corneal edema.

The role of DNA methyltransferase 1 in eyelid morphogenesis: A massive morphogenetic event in the late embryonic development of the mammalian eye is closure of the upper and lower eyelids, resulting in an enclosed eyelid covering the corneal surface [27,28]. Mouse eyelid closure occurs between E15.5 and E16.5, and the eyelids remain fused at birth. Thus, mice are normally born with their eyes closed, whereas newborn pups display an “eye-open” at birth (EOB) phenotype when the eyelids fail to fuse prenatally [29]. The observations that eyelids fail to fuse in *Dnmt1*$^{\Delta OSE}$ E16.5 fetuses has led us to ask whether this defect resulted ultimately in the EOB phenotype. To address the question, we examined E17.5,

E18.5 and postnatal day 1 (P1) pups and found that, unlike wild-type mice, which had fully closed eyelids, *Dnmt1*$^{\Delta OSE}$ pups had partially open eyelids (Figure 4).

Prior to eyelid closure, the peridermal cells at the eyelid tip undergo morphological changes, leading to the formation of a protrusion that presumably initiates the centripetal epithelial movement for lid closure [30]. To understand how *Dnmt1* knockout impairs closure, we examined the tips of wild-type and *Dnmt1*$^{\Delta OSE}$ eyelids at E15.5, a developmental stage at the onset of lid closure. Eyelid tip epithelial protrusion was evident in the wild-type but not the knockout embryos (arrowhead, Figure 5A). The knockout eyelid tip instead appeared to fold posteriorly and became thicker (asterisk, Figure 5A); its epithelial cells were less compact with larger intercellular spaces, and some of the suprabasal cells had condensed chromatin (arrows, Figure 5A). Similar

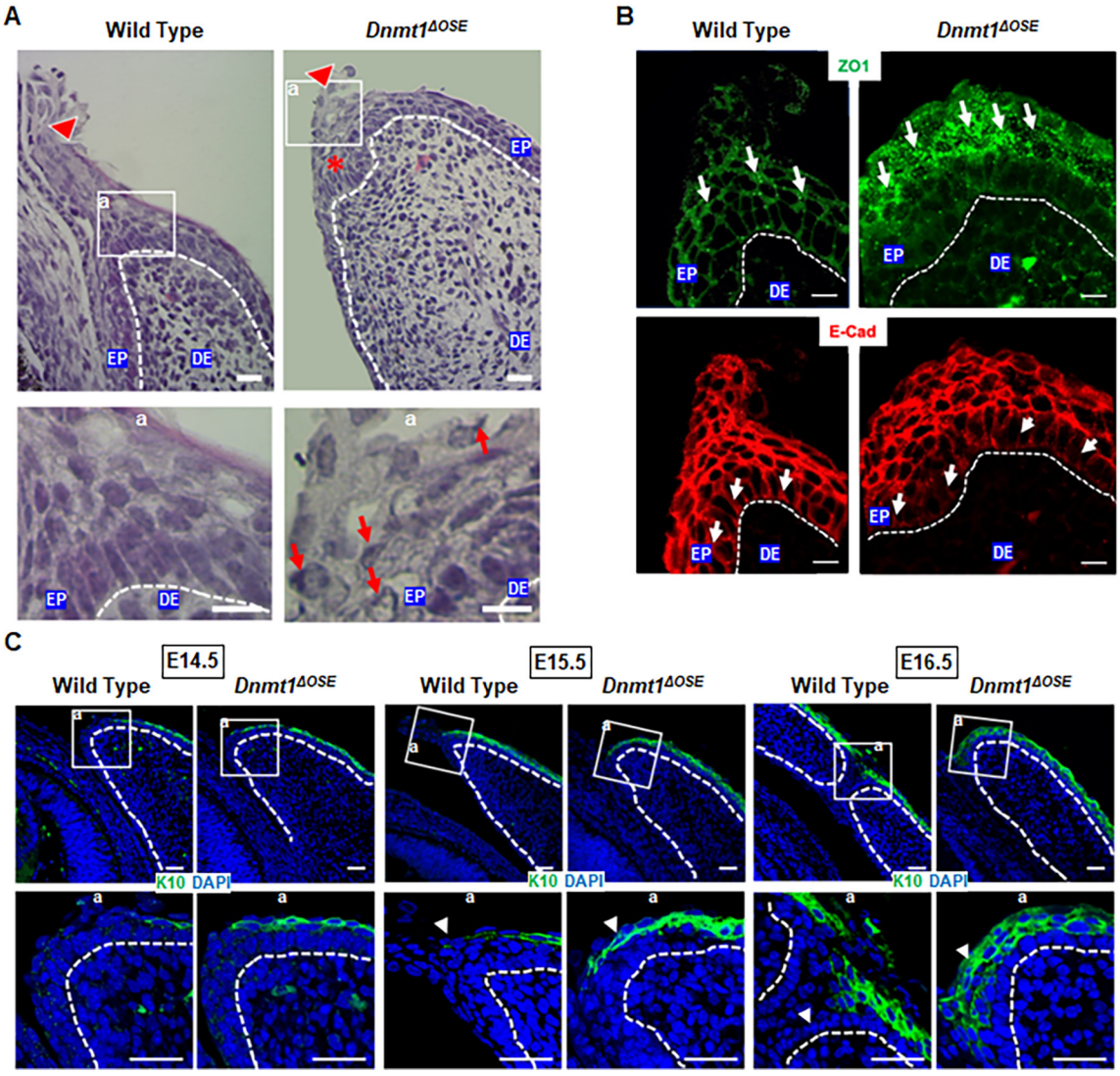

Figure 5. DNA methyltransferase 1 ablation disrupts eyelid morphology and differentiation. **A**: Wild-type and *Dnmt1*$^{\Delta OSE}$ E15.5 embryonic eye sections were subjected to Hematoxylin and eosin staining, and eyelid tip images were captured at lower (upper panels) and higher magnifications of the selected areas (a, lower panels). Arrowheads point to the epithelial protrusion of the eyelid tip, asterisks mark eyelid epithelial folding and arrows indicate cells displaying condensed nuclei in the *Dnmt1*$^{\Delta OSE}$ eyelids. **B**: Immunostaining using anti-E-Cad and anti-ZO-1, as indicated. Arrows point to abnormal ZO-1 localization and reduced E-Cad in the *Dnmt1*$^{\Delta OSE}$ eyelids. **C**: Wild-type and *Dnmt1*$^{\Delta OSE}$ embryonic eyelids at embryonic days indicated were subjected to immunostaining with anti-K10 for epithelial terminal differentiation. Images were taken at low magnification (upper panels) and high magnification of selected areas (a, lower panels). Arrowheads point to different K10 expression between wild-type and *Dnmt1*$^{\Delta OSE}$ eyelid tips. Dashed lines indicate the epithelial basement membrane. Images are representative of at least three mice/genotypes. Scale bars: 10 µm for (**A**) and (**B**). Scale bars: 30 µm for (**C**). EP, epithelium; DE, dermis.

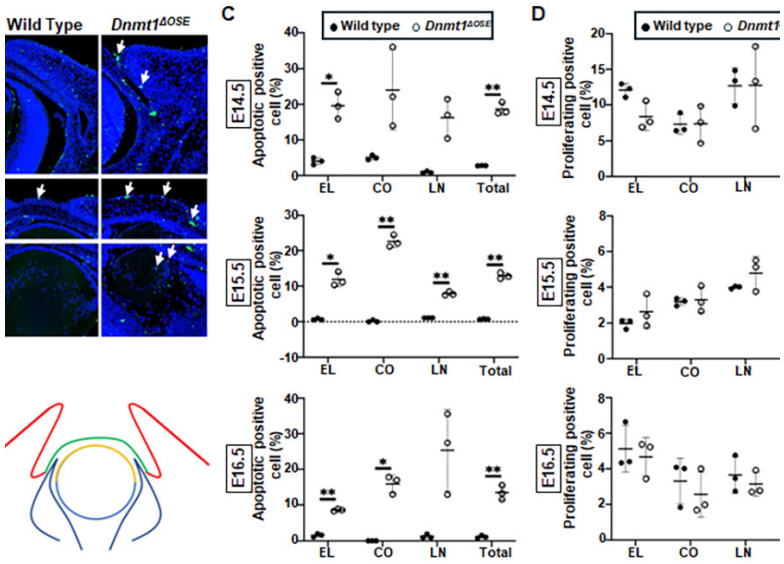

Figure 6. Apoptosis and proliferation in wild-type and *Dnmt1*$^{\Delta OSE}$ embryos. **A**: Representative images of the terminal deoxynucleotidyl transferase dUTP nick-end labeling assay showing apoptotic cells (green, arrows) in different regions of the ocular surface epithelium. **B**: Illustration of the epithelial regions for the eyelids (red), cornea (green) and lens (yellow) used for quantification. Quantification of (**C**) apoptotic cells and (**D**) proliferating cells in the different regions of the ocular surface epithelium in E14.5–E16.5 embryos. EL, Eyelid; CO, Cornea; LN, Lens. Values are mean ± s.e.m. of three embryos/genotype. *p < 0.05, **p < 0.01 (two-tailed Student *t* test).

abnormalities were observed in the eyelid tip of E14.5 and E16.5 *Dnmt1*$^{\Delta OSE}$ embryos (Appendix 4), indicating that DNMT1 ablation prevented the normal formation of eyelid tip protrusion.

To determine if DNMT1 ablation impaired the structural integrity of the eyelid tip like that seen in the cornea, we assessed E-Cad and ZO-1 via immunohistochemistry. Both ZO-1 and E-Cad were detected in the knockout eyelids, but their distributions were somewhat different from that of wild-type eyelids (Figure 5B). In the wild-type eyelid tips, ZO-1 was evenly distributed on the plasma membrane of basal and suprabasal epithelial cells, but in *Dnmt1*$^{\Delta OSE}$ it was scattered throughout the cytosol in the suprabasal cells (asterisk, Figure 5B). E-Cad, on the other hand, was located on the plasma membrane of the eyelid tip epithelial cells in both genotypes, although it appeared to be less abundant in the basal epithelial cells of the knockout eyelids.

The embryonic eyelid is composed of stroma covered by epidermal layers at the anterior surface and conjunctival epithelium on the posterior side [31]. To assess the roles of DNMT1 in anterior and posterior eyelid epithelial differentiation, we determined the expression of K14, a marker of basal proliferative keratinocytes, and K10, which is expressed only in terminally differentiated suprabasal keratinocytes [25]. K14 expression was detected in the basal epithelial cells on both anterior and posterior surfaces of the eyelids, with no major differences observed between wild-type and *Dnmt1*$^{\Delta OSE}$ E14.5–E16.5 embryos (Appendix 5). K10 was detected in the suprabasal layers of the anterior epithelium, and the level of expression gradually increased as the embryos grew older (arrowheads, Figure 5C). Compared with wild-type eyelids, *Dnmt1*$^{\Delta OSE}$ eyelids showed increased K10 expression, both in intensity and in cell layers. In particular, eyelid tip cells were K10-negative in wild-type embryos but became K10-positive in *Dnmt1*$^{\Delta OSE}$ embryos. Thus, DNMT1 loss impairs lid closure through potentiating differentiation and blocking the protrusion of lid tip epithelial cells.

DNA methyltransferase 1 regulates cell proliferation and apoptosis: Because DNMT1 has been shown to regulate proliferation and apoptosis in many organ-formation processes [11,32], we determined these roles in the OSE of E14.5 to E16.5 embryos. An EdU labeling assay was used to assess proliferation and a terminal deoxynucleotidyl transferase dUTP nick-end labeling assay was used to determine apoptosis. Quantification of the labeling data showed that DNMT1 ablation did not change proliferation but increased apoptosis in the OSE (Figure 6A–D). The number of apoptotic cells in all ocular surface epithelia, including the eyelid (EL), cornea (CO) and lens (LN), was significantly higher in *Dnmt1*$^{\Delta OSE}$ than in wild-type embryos. The eyelid tip of the knockout, but not wild-type, embryos showed abundant apoptotic cells, corroborated with histological data showing cells

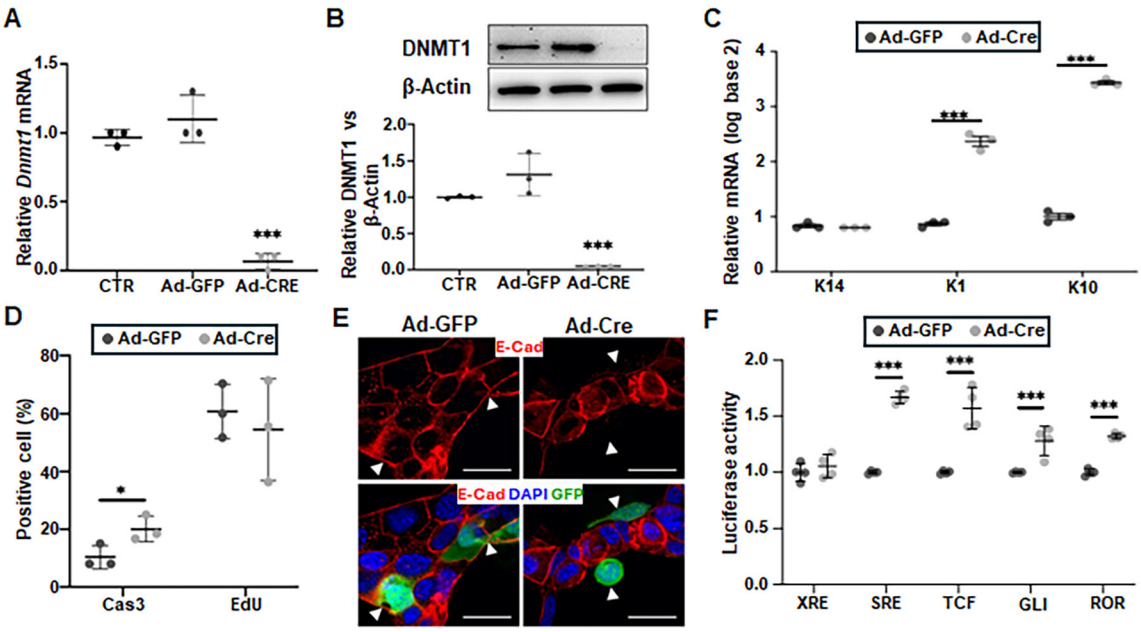

Figure 7. The role of DNMT1 in cultured keratinocytes. *Dnmt1*$^{F/F}$ keratinocytes infected with Ad-GFP or Ad-Cre were examined for (**A**) *Dnmt1* mRNA and (**C**) *K14*, *K1* and *K10* mRNA, normalized by mRNA of *Gapdh*. (**B**) DNMT1 protein normalized by β-actin. **D**: The percentage of apoptosis and proliferation quantified by immunolabelling with anti-Cas-3 and anti-EdU assays, respectively. **E**: Immunofluorescent staining using anti-E-cadherin (E-Cad). Arrowhead points to Ad-GFP/Ad-GFP-Cre–infected cells. Scale bar: 30 µm. **F**: *Dnmt1*$^{F/F}$ reporter stable cells were infected with Ad-GFP or Ad-Cre, and luciferase activities were normalized by total protein. Values are mean ± s.e.m. of three wells/adenovirus. *p < 0.05, ***p < 0.001 (two-tailed Student *t* test).

with condensed nuclei in this region (Figure 5A and Figure 6B). The knockout corneas, on the other hand, displayed increased apoptosis of basal epithelial cells located between the epithelial layer and the stroma (Appendix 6). Neither proliferation nor apoptosis was altered in the stroma of the *Dnmt1*$^{\Delta OSE}$ ocular surface (Appendix 7). These observations suggest that DNMT1 is required for the survival of corneal and eyelid epithelia, like that established previously in the lens epithelium [15].

DNA methyltransferase 1 regulates molecular and cellular activities in cultured keratinocytes: To investigate the roles of DNMT1 in epithelial development in vitro, we isolated epithelial cells from the skin of *Dnmt1*$^{F/F}$ mice and developed keratinocyte lines using a protocol we have recently developed to obtain epidermal stem cell-like characteristics and extensive subculture capacity [20]. Infection of the cells with Ad-Cre resulted in a marked reduction in DNMT1 mRNA and protein, whereas infection with Ad-GFP did not have such an effect (Figure 7A,B). When placed in differentiation media, Ad-GFP– and Ad-Cre–infected *Dnmt1*$^{F/F}$ cells showed the same level of K14 expression; however, Ad-Cre–infected cells, but not Ad-GFP–infected cells, exhibited higher expression of K1 and K10, indicating terminal epidermal differentiation (Figure 7C). Additionally, compared with Ad-GFP–infected cells, Ad-Cre infection significantly increased active Caspase-3 positive cells, suggesting increased apoptosis, without an apparent change in EdU positivity for proliferation (Figure 7D).

To address whether DNMT1 ablation disrupted cell–cell junctions in vitro, as seen in the OSE, we infected *Dnmt1*$^{F/F}$ cells with Ad-GFP and Ad-Cre, and examined E-Cad expression and localization. Clear E-Cad localization was detected on the plasma membrane in Ad-GFP–infected cells, but it disappeared in Ad-Cre–infected cells (Figure 7E). Additionally, in contrast to neighboring Ad-Cre–negative cells displaying regular epithelial morphology with polygonal shapes, Ad-Cre–positive cells lost their epithelial shape and became either round or stretched.

Taking advantage of the easily manipulatable feature of cultured keratinocytes, we further explored the signaling pathways affected by DNMT1 loss. To achieve this, we made stable *Dnmt1*$^{F/F}$ cells carrying luciferase reporters for specific signaling pathways. Infection of the stable cells with Ad-Cre significantly increased SRE-luc activities for MAPK signaling, TCF-luc for WNT signaling, RORγ for retinoic acid signaling and Gli-luc for Hedgehog signaling compared with those infected with Ad-GFP (Figure 7F). On the other hand,

neither Ad-Cre nor Ad-GFP infection changed the activities of XRE-luc for AhR signaling, suggesting that DNMT1 loss led to the activation of specific signaling and transcription programs.

DISCUSSION

Due to its crucial role in global DNA methylation, DNMT1 has been extensively studied in the development of different embryonic tissues that involve dynamic reprograming of the epigenome [11,13,14,33–35]. Here we determined the developmental roles of DNMT1 in previously unexplored tissues, i.e., the OSE cells of the cornea and eyelid. We showed that DNMT1 is required for survival and proper differentiation of the OSE to maintain structural integrity and morphogenesis, and its ablation in OSE leads to corneal edema and eyelid closure defects in the late phase of embryogenesis. These observations suggest that DNMT1 deficiency could be one of the mechanisms underlying congenital corneal dystrophy and eyelid anomaly [36,37].

In the cornea, DNMT1 ablation severely impairs the epithelial architecture, resulting in a loss of cell–cell junctions and distorted cell structure and organization. The basal epithelium of *Dnmt1*$^{\Delta OSE}$ corneas has increased apoptosis along with loss of adherent junctions in the cell–cell and cell–basement membrane interface. These events, as well as the lack of K12 expression, are likely responsible for a disintegrated and leaking epithelium, resulting in a thicker stroma and edema of the cornea. Increased apoptosis may also cause the loss of adherence junctions, although DNMT1 depletion could directly disrupt adherence junctions through activation of SNAIL for transcriptional repression of E-Cad expression [38,39]. Like in corneal epithelia, DNMT1 depletion has been shown to potentiate apoptosis in other cell types, and it may be doing so through activation of p53 to initiate the apoptotic pathway [5,15]. DNMT1 deficiency also leads to massive apoptosis of the lens epithelium [15], and this lens damage may further potentiate persistent hyaloid vascular cell accumulation at posterior to the *Dnmt1*$^{\Delta OSE}$ lens [40].

The structural abnormalities of *Dnmt1*$^{\Delta OSE}$ corneas and eyelids corresponded to increased apoptosis of epithelial cells. DNMT1 is well known as a negative regulator of apoptosis [41], and its repression leads to rapid loss of DNA methylation and subsequent cell death through hypomethylation of pro-apoptotic genes, widespread DNA damage and genomic instability [33] [42]. We observed a 10–20% increase in apoptosis in *Dnmt1*$^{\Delta OSE}$ eyelid and corneal epithelia. This level of cell death could be sufficient to create open space to generate mechanical tension and induce shape changes in neighboring cells. The tension may also cause reorganization of the extracellular environment and tissue remodeling [43,44]. Additionally, signaling molecules released from the dead cells may act in trans to influence remodeling and activities of the surrounding cells [45,46]. DNMT1 is a positive regulator of cell proliferation through promoter hypermethylation and downregulation of genes involved in blocking cell cycle progression [47]; however, its knockout in OSE does not appear to affect proliferation in the cornea and eyelids, as well as the lens [15]. It is possible that the proliferation program of OSE is less susceptible to DNMT1 loss in contrast to the survival program, which is sensitive to disruption by DNMT1 deficiency.

DNA methylation is a key regulator of differentiation through distinct methylation patterns to establish the unique identity of differentiated cell types [48,49]. Here we showed that DNMT1 is dispensable for the differentiation of K14-positive basal epithelia but has distinct effects on terminal differentiation of cornea and eyelid epithelia. In the cornea, DNMT1 is essential for the development of K12-positive cells, which are corneal epithelial cells that specify maturation [24,26]. As DNMT1 has been shown to regulate progenitor differentiation in many tissues [14,50,51], its inhibition may occur in corneal progenitors to compromise the differentiation of corneal-specific epithelial cells, leading to diseases such as corneal dystrophy [52,53]. In the eyelid, epidermal terminal differentiation is developmentally accelerated in *Dnmt1*$^{\Delta OSE}$ embryos. These observations are consistent with the established functions of DNMT1 in the epidermis, where it suppresses terminal differentiation through the methylation of epidermal differentiation gene promoters [12]. This accelerated terminal differentiation and increased apoptosis in the eyelid tip of E15.5 embryos may contribute to lid closure defects in the *Dnmt1*$^{\Delta OSE}$ mice.

Cultured murine keratinocytes possess epithelial stem-like features and can be induced into terminal differentiation [20]. This in vitro model is therefore suitable to characterize the roles of DNMT1 in epithelial development because, like in OSE, DNMT1 ablation in these cells potentiates differentiation and apoptosis, and disrupts adherence junctions. Moreover, DNMT1 ablation in these cells led to the activation of some, but not all, signaling reporters, suggesting that reporter activation was not due to nonspecific global promoter hypomethylation. Some activated signaling pathways may contribute to the eye phenotypes seen in *Dnmt1*$^{\Delta OSE}$ embryos. Hyperactivation of WNT signaling, for example, disrupts eyelid and corneal morphogenesis during mouse embryonic development and perturbs cell proliferation and differentiation of the epithelium [54]. Similarly, excessive activation of the growth factor receptor/SRE pathway leads to aberrant

differentiation and morphogenesis of multiple ocular cell types/tissues [55,56], whereas overactivation of Hedgehog signaling impairs cell motility, morphology and developmental eye tissue closure [57]. Thus, DNMT1 loss may activate multiple signaling pathways to derail differentiation, apoptosis and morphogenetic programs. As DNMT1 activities can be manipulated through diet [58] and environmental factors [59], understanding its roles in eye development could lead to development of strategies in disease prevention and treatment.

APPENDIX 1. SUPPLEMENTARY TABLE 1.

To access the data, click or select the words "Appendix 1."

APPENDIX 2. SUPPLEMENTARY TABLE 2.

To access the data, click or select the words "Appendix 2."

APPENDIX 3. SUPPLEMENTARY TABLE 3.

To access the data, click or select the words "Appendix 3."

APPENDIX 4. SUPPLEMENTARY FIGURE 1.

To access the data, click or select the words "Appendix 4."

APPENDIX 5. SUPPLEMENTARY FIGURE 2.

To access the data, click or select the words "Appendix 5."

APPENDIX 6. SUPPLEMENTARY FIGURE 3.

To access the data, click or select the words "Appendix 6."

APPENDIX 7. SUPPLEMENTARY FIGURE 4.

To access the data, click or select the words "Appendix 7."

ACKNOWLEDGMENTS

The work was supported in part by National Institute of Health grants RO1HD098106 (YX) and R21ES033342 (YX).

REFERENCES

1. Jin B, Li Y, Robertson KD. DNA methylation: superior or subordinate in the epigenetic hierarchy? Genes Cancer 2011; 2:607-17. [PMID: 21941617].
2. Bird A. DNA methylation patterns and epigenetic memory. Genes Dev 2002; 16:6-21. [PMID: 11782440].
3. Bernstein BE, Kamal M, Lindblad-Toh K, Bekiranov S, Bailey DK, Huebert DJ, McMahon S, Karlsson EK, Kulbokas EJ 3rd, Gingeras TR, Schreiber SL, Lander ES. Genomic maps and comparative analysis of histone modifications in human and mouse. Cell 2005; 120:169-81. [PMID: 15680324].
4. Kikuchi A, Onoda H, Yamaguchi K, Kori S, Matsuzawa S, Chiba Y, Tanimoto S, Yoshimi S, Sato H, Yamagata A, Shirouzu M, Adachi N, Sharif J, Koseki H, Nishiyama A, Nakanishi M, Defossez PA, Arita K. Structural basis for activation of DNMT1. Nat Commun 2022; 13:7130-[PMID: 36414620].
5. Egger G, Jeong S, Escobar SG, Cortez CC, Li TW, Saito Y, Yoo CB, Jones PA, Liang G. Identification of DNMT1 (DNA methyltransferase 1) hypomorphs in somatic knockouts suggests an essential role for DNMT1 in cell survival. Proc Natl Acad Sci U S A 2006; 103:14080-5. [PMID: 16963560].
6. Uysal F, Sukur G, Cinar O. DNMT enzymes differentially alter global DNA methylation in a stage-dependent manner during spermatogenesis. Andrologia 2022; 54:e14357[PMID: 34997784].
7. Heard E. Delving into the diversity of facultative heterochromatin: the epigenetics of the inactive X chromosome. Curr Opin Genet Dev 2005; 15:482-9. [PMID: 16107314].
8. Martienssen R, Lippman Z, May B, Ronemus M, Vaughn M. Transposons, tandem repeats, and the silencing of imprinted genes. Cold Spring Harb Symp Quant Biol 2004; 69:371-9. [PMID: 16117670].
9. Li E, Bestor TH, Jaenisch R. Targeted mutation of the DNA methyltransferase gene results in embryonic lethality. Cell 1992; 69:915-26. [PMID: 1606615].
10. Liu R, Kim KY, Jung YW, Park IH. Dnmt1 regulates the myogenic lineage specification of muscle stem cells. Sci Rep 2016; 6:35355-[PMID: 27752090].
11. Elliott EN, Sheaffer KL, Schug J, Stappenbeck TS, Kaestner KH. Dnmt1 is essential to maintain progenitors in the perinatal intestinal epithelium. Development 2015; 142:2163-72. [PMID: 26023099].
12. Sen GL, Reuter JA, Webster DE, Zhu L, Khavari PA. DNMT1 maintains progenitor function in self-renewing somatic tissue. Nature 2010; 463:563-7. [PMID: 20081831].
13. Nasonkin IO, Merbs SL, Lazo K, Oliver VF, Brooks M, Patel K, Enke RA, Nellissery J, Jamrich M, Le YZ, Bharti K, Fariss RN, Rachel RA, Zack DJ, Rodriguez-Boulan EJ, Swaroop A. Conditional knockdown of DNA methyltransferase 1 reveals a key role of retinal pigment epithelium integrity in photoreceptor outer segment morphogenesis. Development 2013; 140:1330-41. [PMID: 23406904].
14. Rhee KD, Yu J, Zhao CY, Fan G, Yang XJ. Dnmt1-dependent DNA methylation is essential for photoreceptor terminal differentiation and retinal neuron survival. Cell Death Dis 2012; 3:e427[PMID: 23171847].
15. Hoang TV, Horowitz ER, Chaffee BR, Qi P, Flake RE, Bruney DG, Rasor BJ, Rosalez SE, Wagner BD, Robinson ML. Lens development requires DNMT1 but takes place normally in the absence of both DNMT3A and DNMT3B activity. Epigenetics 2017; 12:27-40. [PMID: 27824296].
16. Chow RL, Lang RA. Early eye development in vertebrates. Annu Rev Cell Dev Biol 2001; 17:255-96. [PMID: 11687490].

17. Azuma N, Yamaguchi Y, Handa H, Tadokoro K, Asaka A, Kawase E, Yamada M. Mutations of the PAX6 gene detected in patients with a variety of optic-nerve malformations. Am J Hum Genet 2003; 72:1565-70. [PMID: 12721955].

18. Mihelec M, St Heaps L, Flaherty M, Billson F, Rudduck C, Tam PP, Grigg JR, Peters GB, Jamieson RV. Chromosomal rearrangements and novel genes in disorders of eye development, cataract and glaucoma. Twin Res Hum Genet 2008; 11:412-21. [PMID: 18637741].

19. Reis LM, Semina EV. Conserved genetic pathways associated with microphthalmia, anophthalmia, and coloboma. Birth Defects Res C Embryo Today 2015; 105:96-113. [PMID: 26046913].

20. Wang J, Mongan M, Zhang X, Xia Y. Isolation and long-term expansion of murine epidermal stem-like cells. PLoS One 2021; 16:e0254731[PMID: 34270586].

21. Ashery-Padan R, Marquardt T, Zhou X, Gruss P. Pax6 activity in the lens primordium is required for lens formation and for correct placement of a single retina in the eye. Genes Dev 2000; 14:2701-11. [PMID: 11069887].

22. Hartsock A, Nelson WJ. Adherens and tight junctions: structure, function and connections to the actin cytoskeleton. Biochim Biophys Acta 2008; 1778:660-9. [PMID: 17854762].

23. Schneeberger EE, Lynch RD. The tight junction: a multifunctional complex. Am J Physiol Cell Physiol 2004; 286:C1213-28. [PMID: 15151915].

24. Tanifuji-Terai N, Terai K, Hayashi Y, Chikama T, Kao WW. Expression of keratin 12 and maturation of corneal epithelium during development and postnatal growth. Invest Ophthalmol Vis Sci 2006; 47:545-51. [PMID: 16431949].

25. Byrne C, Tainsky M, Fuchs E. Programming gene expression in developing epidermis. Development 1994; 120:2369-83. [PMID: 7525178].

26. Kurpakus MA, Maniaci MT, Esco M. Expression of keratins K12, K4 and K14 during development of ocular surface epithelium. Curr Eye Res 1994; 13:805-14. [PMID: 7531631].

27. Harris MJ, Juriloff DM. Eyelid development and fusion induced by cortisone treatment in mutant, lidgap-Miller, foetal mice. A scanning electron microscope study. J Embryol Exp Morphol 1986; 91:1-18. [PMID: 3711778].

28. Findlater GS, McDougall RD, Kaufman MH. Eyelid development, fusion and subsequent reopening in the mouse. J Anat 1993; 183:121-9. [PMID: 8270467].

29. Teramoto S, Fujii S, Yoshida A, Shirasu Y. Morphological and genetic characteristics of the open-eyelid mutant spontaneously occurring in NC-strain mice. Jikken Dobutsu 1988; 37:455-62. [PMID: 3149245].

30. Tawfik HA, Abdulhafez MH, Fouad YA, Dutton JJ. Embryologic and Fetal Development of the Human Eyelid. Ophthalmic Plast Reconstr Surg 2016; 32:407-14. [PMID: 27124372].

31. Sevel D. A reappraisal of the development of the eyelids. Eye (Lond) 1988; 2:123-9. [PMID: 3197869].

32. Bai Y, Lang L, Zhao W, Niu R. Long Non-Coding RNA HOXA11-AS Promotes Non-Small Cell Lung Cancer Tumorigenesis Through microRNA-148a-3p/DNMT1 Regulatory Axis. Onco Targets Ther 2019; 12:11195-206. [PMID: 31908486].

33. Liao J, Karnik R, Gu H, Ziller MJ, Clement K, Tsankov AM, Akopian V, Gifford CA, Donaghey J, Galonska C, Pop R, Reyon D, Tsai SQ, Mallard W, Joung JK, Rinn JL, Gnirke A, Meissner A. Targeted disruption of DNMT1, DNMT3A and DNMT3B in human embryonic stem cells. Nat Genet 2015; 47:469-78. [PMID: 25822089].

34. Takebayashi S, Tamura T, Matsuoka C, Okano M. Major and essential role for the DNA methylation mark in mouse embryogenesis and stable association of DNMT1 with newly replicated regions. Mol Cell Biol 2007; 27:8243-58. [PMID: 17893328].

35. Bestor TH. The DNA methyltransferases of mammals. Hum Mol Genet 2000; 9:2395-402. [PMID: 11005794].

36. Weiss JS, Rapuano CJ, Seitz B, Busin M, Kivelä TT, Bouheraoua N, Bredrup C, Nischal KK, Chawla H, Borderie V, Kenyon KR, Kim EK, Møller HU, Munier FL, Berger T, Lisch W. IC3D Classification of Corneal Dystrophies-Edition 3. Cornea 2024; 43:466-527. [PMID: 38359414].

37. Al-Mujaini A, Yahyai MA, Ganesh A. Congenital Eyelid Anomalies: What General Physicians Need To Know. Oman Med J 2021; 36:e279[PMID: 34267952].

38. Espada J, Peinado H, Lopez-Serra L, Setién F, Lopez-Serra P, Portela A, Renart J, Carrasco E, Calvo M, Juarranz A, Cano A, Esteller M. Regulation of SNAIL1 and E-cadherin function by DNMT1 in a DNA methylation-independent context. Nucleic Acids Res 2011; 39:9194-205. [PMID: 21846773].

39. Bowler EH, Smith-Vidal A, Lester A, Bell J, Wang Z, Bell CG, Wang Y, Divecha N, Skipp PJ, Ewing RM. Deep proteomic analysis of Dnmt1 mutant/hypomorphic colorectal cancer cells reveals dysregulation of epithelial-mesenchymal transition and subcellular re-localization of Beta-Catenin. Epigenetics 2020; 15:107-21. [PMID: 31448663].

40. Khokhar S, Dhull C. Commentary: Understanding angiogenic factors in pathogenesis of persistent fetal vasculature. Indian J Ophthalmol 2019; 67:1622-3. [PMID: 31546494].

41. Yan L, Geng Q, Cao Z, Liu B, Li L, Lu P, Lin L, Wei L, Tan Y, He X, Li L, Zhao N, Lu C. Insights into DNMT1 and programmed cell death in diseases. Biomed Pharmacother 2023; 168:115753[PMID: 37871559].

42. Georgia S, Kanji M, Bhushan A. DNMT1 represses p53 to maintain progenitor cell survival during pancreatic organogenesis. Genes Dev 2013; 27:372-7. [PMID: 23431054].

43. Pérez-Garijo A, Steller H. Spreading the word: non-autonomous effects of apoptosis during development, regeneration and disease. Development 2015; 142:3253-62. [PMID: 26443630].

44. Wickman G, Julian L, Olson MF. How apoptotic cells aid in the removal of their own cold dead bodies. Cell Death Differ 2012; 19:735-42. [PMID: 22421963].

45. Essien SA, Ahuja I, Eisenhoffer GT. Apoptotic extracellular vesicles carrying Mif regulate macrophage recruitment and compensatory proliferation in neighboring epithelial stem cells during tissue maintenance. PLoS Biol 2024; 22:e3002194[PMID: 39495793].

46. Pérez-Garijo A, Fuchs Y, Steller H. Apoptotic cells can induce non-autonomous apoptosis through the TNF pathway. Elife 2013; 2:e01004[PMID: 24066226].

47. Baylin SB, Herman JG, Graff JR, Vertino PM, Issa JP. Alterations in DNA methylation: a fundamental aspect of neoplasia. Adv Cancer Res 1998; 72:141-96. [PMID: 9338076].

48. Ehrlich M, Lacey M. DNA methylation and differentiation: silencing, upregulation and modulation of gene expression. Epigenomics 2013; 5:553-68. [PMID: 24059801].

49. O'Neill KM, Irwin RE, Mackin SJ, Thursby SJ, Thakur A, Bertens C, Masala L, Loughery JEP, McArt DG, Walsh CP. Depletion of DNMT1 in differentiated human cells highlights key classes of sensitive genes and an interplay with polycomb repression. Epigenetics Chromatin 2018; 11:12-[PMID: 29598829].

50. Liu J, Banerjee A, Herring CA, Attalla J, Hu R, Xu Y, Shao Q, Simmons AJ, Dadi PK, Wang S, Jacobson DA, Liu B, Hodges E, Lau KS, Gu G. Neurog3-Independent Methylation Is the Earliest Detectable Mark Distinguishing Pancreatic Progenitor Identity. Dev Cell 2019; 48:49-63.e7. [PMID: 30620902].

51. Chappell C, Beard C, Altman J, Jaenisch R, Jacob J. DNA methylation by DNA methyltransferase 1 is critical for effector CD8 T cell expansion. J Immunol 2006; 176:4562-72. [PMID: 16585546].

52. Klintworth GK. Corneal dystrophies. Orphanet J Rare Dis 2009; 4:7-[PMID: 19236704].

53. Irvine AD, Corden LD, Swensson O, Swensson B, Moore JE, Frazer DG, Smith FJ, Knowlton RG, Christophers E, Rochels R, Uitto J, McLean WH. Mutations in cornea-specific keratin K3 or K12 genes cause Meesmann's corneal dystrophy. Nat Genet 1997; 16:184-7. [PMID: 9171831].

54. Mizoguchi S, Suzuki K, Zhang J, Yamanaka O, Liu CY, Okada Y, Miyajima M, Kokado M, Kao WW, Yamada G, Saika S. Disruption of eyelid and cornea morphogenesis by epithelial β-catenin gain-of-function. Mol Vis 2015; 21:793-803. [PMID: 26283861].

55. Makrides N, Wang Q, Tao C, Schwartz S, Zhang X. Jack of all trades, master of each: the diversity of fibroblast growth factor signalling in eye development. Open Biol 2022; 12:210265[PMID: 35016551].

56. Freeman M. Reiterative use of the EGF receptor triggers differentiation of all cell types in the Drosophila eye. Cell 1996; 87:651-60. [PMID: 8929534].

57. Gordon HB, Lusk S, Carney KR, Wirick EO, Murray BF, Kwan KM. Hedgehog signaling regulates cell motility and optic fissure and stalk formation during vertebrate eye morphogenesis. Development 2018; 145:dev165068[PMID: 30333214].

58. da Mota JCNL, Ribeiro AA, Carvalho LM, Esteves GP, Sieczkowska SM, Goessler KF, Gualano B, Nicoletti CF. Impact of Methyl-Donor Micronutrient Supplementation on DNA Methylation Patterns: A Systematic Review and Meta-Analysis of in vitro, Animal, and Human Studies. Lifestyle Genom 2023; 16:192-213. [PMID: 37935134].

59. Keil KP, Lein PJ. DNA methylation: a mechanism linking environmental chemical exposures to risk of autism spectrum disorders? Environ Epigenet 2016; 2:dvv012[PMID: 27158529].

Articles are provided courtesy of Emory University and The Abraham J. & Phyllis Katz Foundation. The print version of this article was created on 28 March 2025. This reflects all typographical corrections and errata to the article through that date. Details of any changes may be found in the online version of the article.